IMPLICATIONS OF CUMULATED SEISMIC DAMAGE ON THE SEISMIC PERFORMANCE OF UNREINFORCED MASONRY BUILDINGS

Amaryllis Mouyiannou[1], Andrea Penna[2], Maria Rota[3], Francesco Graziotti[4] and Guido Magenes[5]

SUMMARY

The seismic capacity of a structure is a function of the characteristics of the system as well as of its state, which is mainly affected by previous damage and deterioration. The cumulative damage from repeated shocks (for example during a seismic sequence or due to multiple events affecting an unrepaired building stock) affects the vulnerability of masonry buildings for subsequent events. This paper proposes an analytical methodology for the derivation of state-dependent fragility curves, taking into account cumulated seismic damage, whilst neglecting possible ageing effects. The methodology is based on nonlinear dynamic analyses of an equivalent single degree of freedom system, properly calibrated to reproduce the static and dynamic behaviour of the structure. An application of the proposed methodology to an unreinforced masonry case study building is also presented. The effect of cumulated damage on the seismic response of this prototype masonry building is further studied by means of nonlinear dynamic analyses with the accelerograms recorded during a real earthquake sequence that occurred in Canterbury (New Zealand) between 2010 and 2012.

1. INTRODUCTION

The seismic vulnerability of a masonry building depends on several structural characteristics, including structural materials, dressing and layout of masonry units, presence of seismic elements (e.g. tie rods and tie beams), number of storeys, diaphragm in-plane flexibility [1,2]. This intrinsic vulnerability of masonry buildings is then further affected by the state of the structure, in terms of previous damage and conservation/deterioration. The latter may be related to either natural or anthropic causes, to continuous and long duration phenomena or, otherwise, to isolated and rare events. Obviously, the state-dependency of the vulnerability has to be taken into account when estimating the seismic safety of a building.

Seismic events are among the most relevant causes of damage to structural and non-structural components of a building and hence they affect the seismic vulnerability of structures with respect to possible future earthquakes. This aspect is particularly relevant in the time period of a seismic sequence, during which a series of repeated shaking of different severity affects a previously damaged and unrepaired building stock. Several cases of such cumulated damage during seismic sequences have been observed all over the world, also during recent seismic events, such as for example in Emilia (Italy, 2012) and New Zealand (2010-2012), as documented for example in [3] for the Emilia event and [4,5] for the Christchurch sequence.

Therefore, the vulnerability of a structure depends on its damage state, which is a function of the seismic history of the site since the system was established (construction time in case of structures) and of the state of maintenance of the structure. The latter mainly refers to the so-called ageing effects, which are not explicitly considered in this work, but are the subject of ongoing research (e.g. [6,7] for reinforced concrete structures). Similarly, other possible damage apart from those caused by seismic events are not considered in this work, which is focused on the effect of repeated seismic shaking on the vulnerability of masonry buildings. Stochastic modelling of structure deterioration considering the combination of ageing and damage accumulation has also been recently studied with reference to simple elastic-perfectly plastic structural systems [8].

If repair, retrofitting or maintenance interventions are not considered, the seismic safety can be reasonably assumed to decrease with time, due to deterioration. The damage accumulation due to seismic events is by nature a discontinuous process. In general, the effect of the event intensity on the damage evolution and hence on the reduction of the residual capacity is highly nonlinear and only events whose intensity at the site exceeds a certain threshold affect damage accumulation and hence the state of the structures. Such an intensity threshold can be regarded itself as a function of the previous damage state.

The safety of a building, i.e. its capacity to withstand a certain level of seismic action, can be expressed in terms of the so-called intensity measures (IMs), which can be either scalar or

[1]*PhD student, ROSE program ,UME School, IUSS, Pavia*

[2]*Assistant Professor, Department of Civil Engineering and Architecture, University of Pavia, Pavia*

[3]*Researcher, European Centre for Training and Research in Earthquake Engineering, Pavia*

[4]*Post-doc, European Centre for Training and Research in Earthquake Engineering, Pavia*

[5]*Associate Professor, Department of Civil Engineering and Architecture, University of Pavia, Pavia*

vector parameters (e.g. [9] for the use of vector IMs). Since seismic safety has to be evaluated for different limit states, the seismic capacity can be expressed by a set of values of the selected IMs, corresponding to the levels of seismic action inducing the attainment of the considered limit states, i.e. the attainment of given thresholds for selected engineering demand parameters (EDPs).

Based on the aforementioned considerations, the problem of defining time-dependent vulnerability of systems can be split into two separate sub-problems:

1. Definition of the system state as a function of time, e.g. considering the combined effect of ageing and cumulated seismic damage.
2. Definition of state-dependent fragility curves representing the seismic vulnerability of the system for a given system state (at a given time).

The first aspect is explicitly considered in some literature works, either only referring to the co-seismic accumulation of damage [10] or more in general [11]. On the other hand, the evaluation of state-dependent vulnerability of structures can be found for example in [12-13], with reference to reinforced concrete structures.

Several studies on the effect of multiple shaking on the seismic response of structures can be found in the literature, either with reference to SDOF systems [14-16] or MDOF reinforced concrete [17-19] and steel structures [20].

The issue of the seismic assessment of damaged buildings was the subject of forerunning FEMA documents [21-22], which were published a few years ago and included only limited information relevant for unreinforced masonry buildings.

This article aims at investigating the influence of the damage state on the seismic vulnerability of unreinforced masonry buildings, by studying the increased seismic demand of structures which have experienced previous earthquakes (inducing a level of pre-damage to the structure) if compared to undamaged or less damaged ones. The vulnerability of the pre-damaged structures cannot be represented by conventional fragility curves derived from analyses of undamaged structural models. The effect of pre-existing damage should be accounted for by means of appropriate state-dependent fragility curves, specifically derived for previously damaged buildings.

A procedure for the derivation of state-dependent fragility functions for buildings with a given (cumulated) seismic damage is proposed in this the paper. The main steps of this procedure consist of:

1. Selection of representative models for each considered building typology (e.g. identification of representative building prototypes and modelling strategies);
2. Collection of experimental information on the mechanical properties of each considered masonry typology;
3. Selection of seismic input for time-history analysis, which is a non-trivial aspect, as discussed for example in [23-25];
4. Selection of relevant engineering demand parameters (EDPs);
5. Identification of relevant limit states and corresponding EDP thresholds. The definition of limit states from the results of time-history analyses is still a debatable issue, as discussed in [26]. EDP thresholds can be selected based on experimental results [27];
6. Derivation of pre-damaged models by imposing different damage conditions in terms of increasing values of the selected EDP;
7. Analytical derivation of fragility functions for pre-damaged models.

The state-dependent fragility curves developed according to the proposed procedure can be representative of the vulnerability of structures in case of repeated events such as aftershocks and they can be used for risk assessment, if combined with aftershock probabilistic seismic hazard assessment. The results of such aftershock risk assessment, referred also as short-term risk assessment, can be helpful for stake-holders and decision makers in order to perform building tagging and monitor the structural risk after the occurrence of a seismic event [28-29]. A closed-form procedure for aftershock reliability has recently been developed for damage-cumulating elasto-perfectly-plastic systems, for which closed-form approximations are derived for the probability of failure of mainshock-damaged structures exposed to following aftershocks [11].

The derived state-dependent fragility curves can be used for complete risk assessments, whose results need to be validated. As an example, the outcome of the analytical assessment procedures based on the use of state-dependent fragility curves could be compared with the results (in terms of seismic demand) of nonlinear time-history analyses with the records of real sequences. Studying the case of a real sequence allows indeed a better understanding of how the cumulated damage is affecting the vulnerability of a structure in the subsequent events. To this aim, the paper discusses the results obtained for the same structural models used for the derivation of state-dependent fragility curves, subjected to the records of the Canterbury earthquake sequence (New Zealand, 2010-2012).

It should be remarked that the aim of this paper is methodological and the analysed case study building was simply selected to show the applicability of the proposed approach. In order to obtain results which are consistent with the characteristics of the New Zealand building stock, detailed information on the prevailing building typologies is needed [30].

Moreover, for the purpose of this study the sole global response governed by the in-plane wall behaviour is considered. In existing masonry buildings, the lack of appropriate structural details and the presence of poor connections between orthogonal walls and between walls and floors often induces local collapses, typically associated with the wall out-of-plane response. Despite this source of vulnerability is recognized as very important and has to be carefully considered in the seismic assessment of masonry structures, it seems to be less dependent on the effect of cumulated damage due to previous seismic events. Indeed, once the mechanism is triggered, the seismic response of masonry portions involved in local failure modes is usually governed by a rocking behaviour with little degradation associated with repeated shaking [31-32]. For the assessment of the effective vulnerability of a real building, the cumulated damage associated with the in-plane response, according to the methodology proposed in this paper, should be combined with the vulnerability resulting from local/out-of-plane mechanisms.

2. PROPOSED PROCEDURE FOR THE DERIVATION OF STATE-DEPENDENT FRAGILITY CURVES

The procedure for deriving state-dependent fragility curves for masonry buildings is outlined in Figure 1.

The first step consists of the definition of a representative model of the building under study. For the case when state-dependent fragility curves need to be defined for a building

typology, a building prototype should be selected and it should be as representative as possible of the typology of interest. First of all, a multi degree of freedom (MDOF) model of the structure must be created, with material parameters calibrated from experimental data.

The identification of appropriate limit states from the results of nonlinear dynamic analyses is a very open issue for which a widely accepted solution is still not available [33]. Although an attempt for the case of masonry structures can be found in [26], in the proposed procedure the limit states of interest for the structure are identified from the results of nonlinear static analyses with the MDOF model. This is a practical approach to this unresolved issue, as it is significantly easier to identify meaningful limit states from the results of pushover analysis, rather than directly from time-history analysis results. In the proposed procedure, deterministic limit state thresholds were used, although a statistical definition could be easily implemented in the procedure, as done for example in [27].

In this work, the limit state thresholds were expressed in terms of significant displacements identified on the building capacity curve. In particular, three limit states were considered: operational limit state (OLS), damage limitation limit state (DLS) and ultimate limit state (ULS).

Based on the results of analyses with this MDOF model, a single degree of freedom (SDOF) model can be derived, making sure it is able to correctly reproduce both the monotonic and cyclic response of the structure. If the SDOF model is adequately representative of the considered building, it can be used in the rest of the procedure, allowing the computational time to be significantly reduced with respect to the MDOF model and hence making possible a higher number of time-history analyses. The seismic response of structures is typically represented in terms of an engineering demand parameter (EDP), which should be well correlated to the damage conditions of the structure. In this procedure, the maximum displacement of the SDOF system is adopted as EDP.

As the structural capacity is defined in terms of discrete displacement levels associated with the attainment of selected limit states, the seismic demand is analogously defined in terms of maximum displacements obtained from time-history analyses. In the proposed approach, seismic demand is defined from the results of time-history analyses with a large number of unscaled records selected from the SIMBAD database [25]. The records are classified by means of two intensity measures, consisting of the peak ground acceleration (PGA) and a so-called "modified Housner intensity (mHI)", that will be defined in a following section.

In this procedure, the displacement demand explicitly accounts for the damage that has previously occurred to the structure. This is done by defining several pre-damage states of the building, associated with the attainment of a given maximum lateral displacement, assuming that the damage condition of the structure is synthetically represented by this EDP. The derivation of models with different levels of pre-existing damage is carried out by subjecting the SDOF model of the building to cyclic pushover analyses up to different predefined levels of displacement. Time-history analyses with unscaled natural records are then performed on these pre-damaged models.

The results of the time-history analyses performed with all the models characterised by different levels of pre-existing damage are statistically processed to derive lognormal fragility curves, as a function of the state of the building and in terms of the two considered intensity measures.

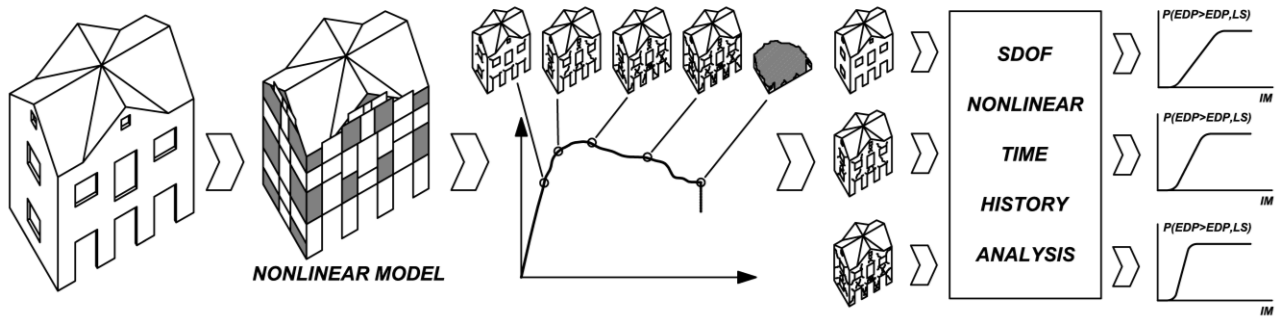

Figure 1: Scheme of the proposed procedure for the derivation of state-dependent fragility curves.

3. EXAMPLE OF APPLICATION TO AN UNREINFORCED MASONRY BUILDING PROTOTYPE

This section presents an example of application of the procedure outlined previously for the derivation of state-dependent fragility curves. After a brief description of the selected building prototype and the calculation of the displacement thresholds corresponding to the three considered limit states, the analyses carried out to generate a set of pre-damaged states for the structure are presented. Then the selection of the records to be used for the time-history analyses performed with the SDOF model is discussed, followed by the results of the nonlinear dynamic analyses. Finally, the fragility curves obtained for the different levels of pre-existing damage are presented and commented.

3.1. Description and modelling of the case study building

The case study building is a two-storey unreinforced clay brick masonry structure, whose geometry was defined starting from the one of a simpler prototype that was subjected to a cyclic quasi-static test at the University of Pavia in 1994 [34]. A MDOF model of the structure (Figure 2**Error! Reference source not found.**) was created using the TREMURI program, an equivalent-frame macro-element program able to perform nonlinear static and dynamic analyses of entire masonry structures [35,36]. The structure was assumed to be realised with the same type of clay brick masonry of the tested specimen. For this reason, the same mechanical parameters of the macro-element model calibrated with reference to the aforementioned experimental results (Figure 3) were used for the case study building.

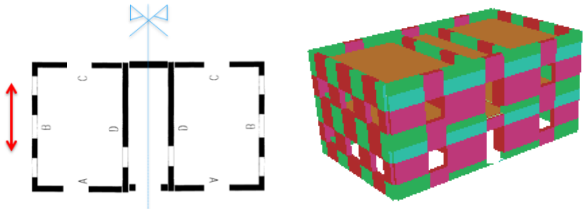

Figure 2: ***Plan and 3D views of the MDOF model of the selected building prototype.***

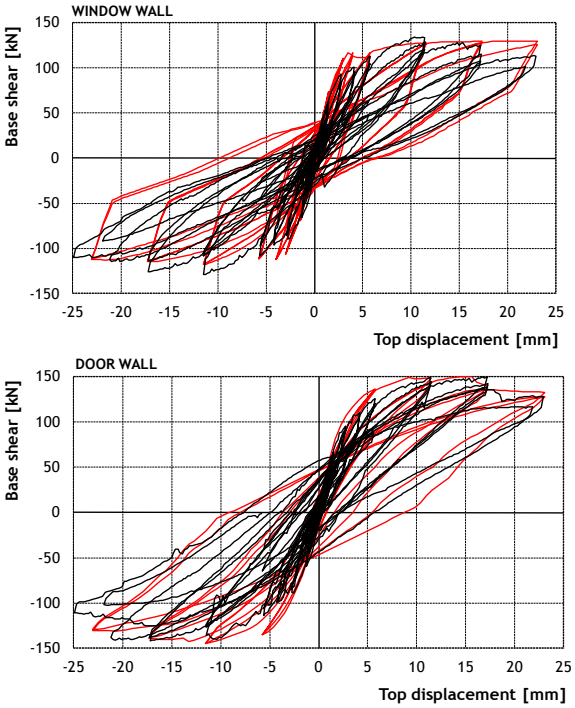

Figure 3: ***Comparison of the force-displacement curves for the two main walls of the full-scale URM building tested by Magenes et al. [34] and corresponding numerical simulation results using the calibrated macro-element model.***

The adopted macro-element model is capable of describing the evolution of flexural and shear cracking for increasing displacement. Therefore, it does not require any a-priori definition of an equivalent cracked stiffness, as it is instead the case for simpler modelling approaches, which are based on an elasto-plastic approximation of the lateral behaviour of masonry walls. In the latter case, values of the equivalent cracked stiffness shall be defined based on the results of experimental tests carried out on a similar masonry typology and can also depend on the level of vertical compression. Typical ratios vary between 50% and 80% of the theoretical stiffness.

The macro-element model was specifically developed for the simulation of the cyclic and dynamic response of masonry buildings and it is also able to reproduce the hysteretic behaviour associated with the in-plane response of masonry walls. For this reason, the energy dissipation associated with material nonlinearity is directly accounted for in the model, and a relatively small value of damping ratio is sufficient to simulate other sources of energy dissipation.

A value of damping ratio between 2% and 5% is commonly adopted, consistently with the experimental results available in the literature [26,37,38] for different types of masonry. In the case of clay brick masonry, it seems appropriate to refer to the lower bound of this range of damping ratios.

Analyses were carried out in the direction indicated by the arrow in the left part of Figure 2. Obviously, a complete seismic assessment of the building would require consideration of at least two orthogonal directions of analysis, but the focus of this work is simply to illustrate the proposed procedure for accounting for cumulated damage.

Based on the results of nonlinear static and dynamic analyses with the MDOF model of the building, a simplified SDOF system, whose behaviour is equivalent to that of the case study building, was calibrated. The scheme adopted for the SDOF model is reported in Figure 4. It can be noted that the system is composed of two two-node macro-elements coupled by an axially rigid link, with the scope of allowing an accurate reproduction of the behaviour of the structure, characterised by a combination of flexural (left macro-element) and shear (right macro-element) responses. The degree of freedom corresponds to the horizontal displacement of the mass on top of the system.

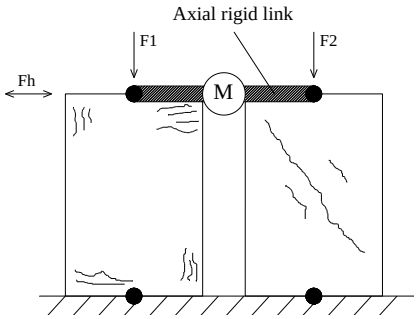

Figure 4: ***SDOF model of the selected building prototype.***

The procedure followed for the static and dynamic calibration of the equivalent SDOF system is described in more detail in Figure 5. In particular, the top part of the figure refers to the static calibration and shows the hysteretic curves obtained by cyclic pushover analysis of the MDOF and SDOF systems, showing a rather good agreement between the results.

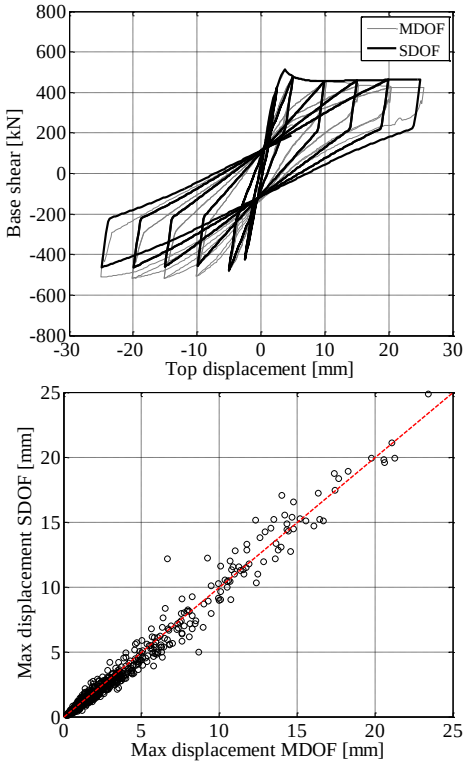

Figure 5: ***Static (top) and dynamic (bottom) calibration of the SDOF model versus the results of the MDOF model.***

The bottom part of Figure 5 instead reports a comparison of the values of displacement obtained from time-history analyses with all the unscaled records of the SIMBAD database, for the SDOF and MDOF systems. It can be seen that the agreement between the two systems is very good, as the results are well aligned along the diagonal.

As discussed in the following sections, this appropriately calibrated SDOF model was then used for the creation of the various levels of the pre-damage of the structure and for the nonlinear dynamic analyses.

3.2. Identification of significant limit states

As mentioned before, the displacement thresholds corresponding to the attainment of the significant limit states considered in the fragility curve derivation were evaluated from nonlinear static analyses with the MDOF model. In particular, the limit states were identified, in terms of displacement thresholds, from the global building capacity (base shear - displacement) curve and from its bilinear idealization. The latter was carried out according to the methodology reported in the Italian building code [40] and described for example in [41-42].

As previously mentioned, three limit states were considered, corresponding to the following displacement thresholds:

1. OLS: the elastic limit of the equivalent bilinear idealization, which for the case study building is equal to 2.3 mm, corresponding to a maximum inter-storey drift of 0.05%;
2. DLS: the displacement corresponding to the attainment of the maximum base shear, which resulted in being equal to 3.8 mm, corresponding to a maximum inter-storey drift of 0.085%;
3. ULS: the displacement corresponding to an 80% degradation of the base shear after its peak, which was found to be equal to 10 mm, corresponding to a maximum inter-storey drift of 0.30%.

In addition to these three limit states, a threshold for a near collapse condition was defined based on experimental evidence as being equal to 25 mm (corresponding to a maximum inter-storey drift of 0.76%). This high displacement level was selected based on the actual maximum displacement imposed to the already mentioned full scale masonry specimen tested under quasi-static conditions [34].

It should be noted that these values of displacement/inter-storey drift limit states refer to the specific masonry typology (clay brick) and building configuration. For applications to other unreinforced masonry types, limit states can be defined in the same way, but the values may be different, due to the different displacement capacity of other masonry typologies [43].

3.3. Generation of pre-damaged states of the structure by cyclic pushover analyses

In order to study the impact of the level of pre-existing damage on the seismic performance of the masonry building, 23 different levels of damage were considered. To obtain the damaged model, the undamaged model was subjected to a cyclic pushover analysis with one cycle, reaching the level of (positive and negative) maximum displacement characterising the damage level. The model with the lowest considered degradation corresponds to a maximum value of displacement equal to 2 mm. Subsequently the models corresponding to increasing levels of pre-damage were derived with values of maximum displacement increasing with a step of 1 mm up to a maximum displacement of 24 mm (pre-collapse condition). It should be noted that these values were obtained for the specific case-study considered in this work. In general, a sufficiently detailed description of the effect of damage evolution can be achieved by considering a suitable number of pre-damage levels regularly spanning from undamaged to near collapse conditions.

Figure 6 shows the cyclic pushover curves for all the derived damage levels. The undamaged structure, corresponding to zero initial damage, is referred as NODAM.

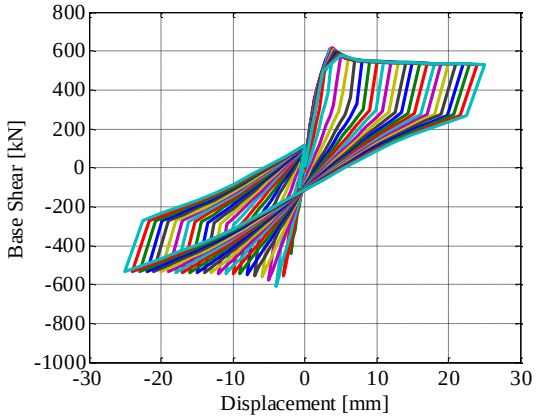

Figure 6: ***Superimposed single-cycle pushover curves of the analyses used to simulate different pre-existing damage levels (indicated by the different colours).***

3.4. Selection of strong-motion records and nonlinear time-history analyses

The earthquake records used for the nonlinear dynamic analyses were selected from the SIMBAD database [25], which includes 467 three-component acceleration records. All the earthquakes have moment magnitude between 5 and 7.3 and epicentral distance not larger than 30 km.

In the presented case study, time-history analyses were performed with unscaled records. To characterise the severity of each accelerogram, it is necessary to select meaningful intensity measures. The first natural choice is to use PGA, as it is a very commonly used parameter for its simplicity of definition and immediate meaning. However, PGA alone is not always able to capture the damage potential of the shaking. When a large number of records is used, it is likely to obtain higher levels of structural damage for higher levels of PGA, but this is not necessarily true for every single earthquake record. For these reasons, in addition to PGA, another intensity measure was adopted for the derivation of state-dependent fragility curves, referred to in the following as modified Housner Intensity (mHI). Housner Intensity is an energy-based intensity measure, calculated for each earthquake record as the integral of the pseudo-velocity spectrum (5% damping) for periods between 0.1 and 2.5 s [44]. This intensity measure was modified by reducing the period range of integration from 0.1 to 0.5 s (as already done in [45]), to better account for the period range of interest for masonry structures, whose effective fundamental period is rarely beyond 0.5 s.

The selection of records from the SIMBAD database was based on considerations on the two selected intensity measures and, in particular, on the values of mHI. The database includes indeed many records with low values of mHI However, preliminary time-history analyses of the case study building showed that records with values of mHI lower than approximately 40 mm are not sufficient to exceed the operational limit state threshold and therefore only a limited number of records in that range were used in the analyses for fragility curves derivation. At the end, 520 earthquake records

were extracted and used for the dynamic analyses with the SDOF model. The two perpendicular horizontal components recorded at the same station for a seismic event were considered as different records for the analyses with the SDOF model.

As shown in Figure 7, the selected records cover in a rather continuous way the range of the two considered intensity measures. The figure also shows that, for a single earthquake record, the two adopted intensity measures are not proportionally related. In other words, a high value of PGA may correspond to a low value of mHI and vice-versa.

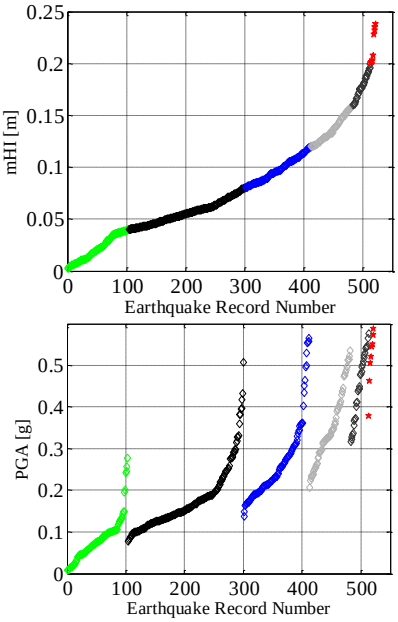

Figure 7: Distribution of the selected earthquake records in terms of the two adopted intensity measures – the colours refer to different ranges of mHI.

Time-history analyses with the undamaged and the 23 pre-damaged models were performed with the unscaled records using the program TREMURI. The large number of analyses required (24 models x 520 records = 12,480 nonlinear dynamic analyses) justifies the use of an equivalent SDOF model which is computationally about 200 times faster than the MDOF model in performing nonlinear dynamic analyses.

Figure 8 shows the values of maximum top displacement of the SDOF model obtained from the time-history analyses, as a function of the two selected intensity measures, for the case of the undamaged structure and for the structure pre-damaged up to a displacement of 9 mm.

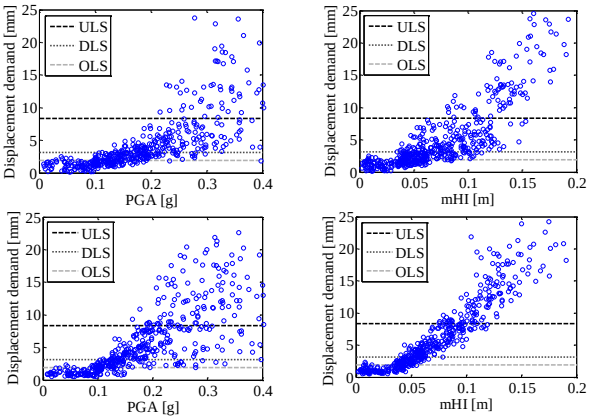

Figure 8: Displacement demand of the SDOF model versus PGA (left) and mHI (right), for the undamaged structure (top) and for the structure pre-damaged up to a displacement of 9 mm (bottom).

The plots also show the displacement thresholds corresponding to the three considered limit states, indicated by horizontal dashed lines. It can be noted that the scatter in the displacement demand is higher in the case where the results are presented in terms of PGA, indicating that mHI is better correlated with the displacement demand. Also, moving from the undamaged to the pre-damaged structure, the scatter is significantly reduced for the case of mHI, whilst the same is not so evident for the case of PGA.

3.5. Derivation of fragility curves and their evolution with pre-existing damage

The maximum displacement demand obtained from the dynamic analyses was compared to the displacement thresholds of the limit states and the probability of exceedance of each limit state was computed for discrete subintervals of the two considered intensity measures. The cumulative probability distributions were then fitted with lognormal curves. The lognormal model is typically adopted in the literature thanks to its simplicity (it only depends on two parameters) and its suitability to represent probability distributions associated with non-negative variables. The lognormal fragility curves obtained for different levels of pre-damage and for the three limit states considered (OLS, DLS and ULS) are presented in Figure 9, as a function of both mHI (top) and PGA (bottom). Each sub-plot of the figure shows 24 curves, corresponding to the results obtained for the 23 pre-damaged structures and the undamaged one.

For OLS, the increase of the level of the pre-existing damage results in an increase of the probability of exceeding the OLS displacement threshold, as expected. This increase is significant, as for example for mHI = 0.05 m the probability of exceeding OLS is 60% for the undamaged model whereas it reaches 83% for the structure pre-damaged to a displacement of 25 mm. The increase is similar for the two different intensity measures considered. The attainment of the OLS is mainly associated with the initial stiffness of the structure and therefore the associated probability is not really sensitive to the selected intensity measure, as evident from Figure 9, where the shape of the fragility curves for OLS is very similar for both PGA and mHI.

The probability of exceeding DLS for a given IM value is also increasing for increasing levels of pre-existing damage. This increase is more pronounced for the lower pre-damage levels. The increase in the probability is different for the different subintervals of each IM. For example, for mHI = 0.05 m, the probability of exceeding DLS increases from 18% for the undamaged structure to 43% for the structure pre-damaged to a 25 mm displacement, whereas for mHI = 0.07 m the probability increases from 40% to 85%.

The probability of exceeding ULS for a given value of mHI is increasing with increasing damage levels up to a pre-damage displacement of 15 mm. For pre-existing damage beyond this level, the fragility curves are similar to each other. In other words, for pre-damage levels higher than 15 mm displacement, the probability of exceeding ULS given a value of mHI is constant with increasing levels of pre-existing damage. For the attainment of ULS, which is controlled by the limited ductility capacity of the system, mHI seems to be a better indicator for the evolution of damage in the highly nonlinear range.

Figure 10 shows the evolution of the values of intensity measure corresponding to a predefined probability of exceedance of the three considered limit state thresholds, as a function of the level of pre-existing damage. In particular, the blue circles correspond to the intensity measure having 50% probability of exceeding each considered limit state (i.e. the median value of the distribution), whereas the red and green

solid markers correspond to the 95% and 5% probability, respectively. The pre-existing damage is represented by a scalar EDP, i.e. the maximum displacement of the cyclic pushover analysis to which the SDOF model was subjected to derive its pre-existing damage. The plots are shown in terms of mHI (top figures) and PGA (bottom figures) and for the thresholds corresponding to OLS, DLS and ULS (from left to right).

In general, as expected, the median value of the IM corresponding to the attainment of any limit state decreases as the level of pre-existing damage increases. The variation of the median values of both the IMs is more pronounced moving to higher limit states (i.e. from OLS to DLS to ULS).

For the OLS and DLS, for a given pre-damage level, the dispersion of the IM values with respect to the median points tends to be higher for the case of mHI, particularly for the lower levels of pre-damage. The opposite occurs for the ULS, for which the dispersion of the PGA values with respect to the median points is really significant and much larger than the corresponding dispersion associated with mHI. This is a further proof of the fact that PGA is not a suitable intensity measure for representing the fragility functions at the higher limit states.

These results show that the choice of an adequate IM is important because it allows a more reliable prediction of the structural behaviour, knowing the characteristics of the expected ground motions in terms of such IM.

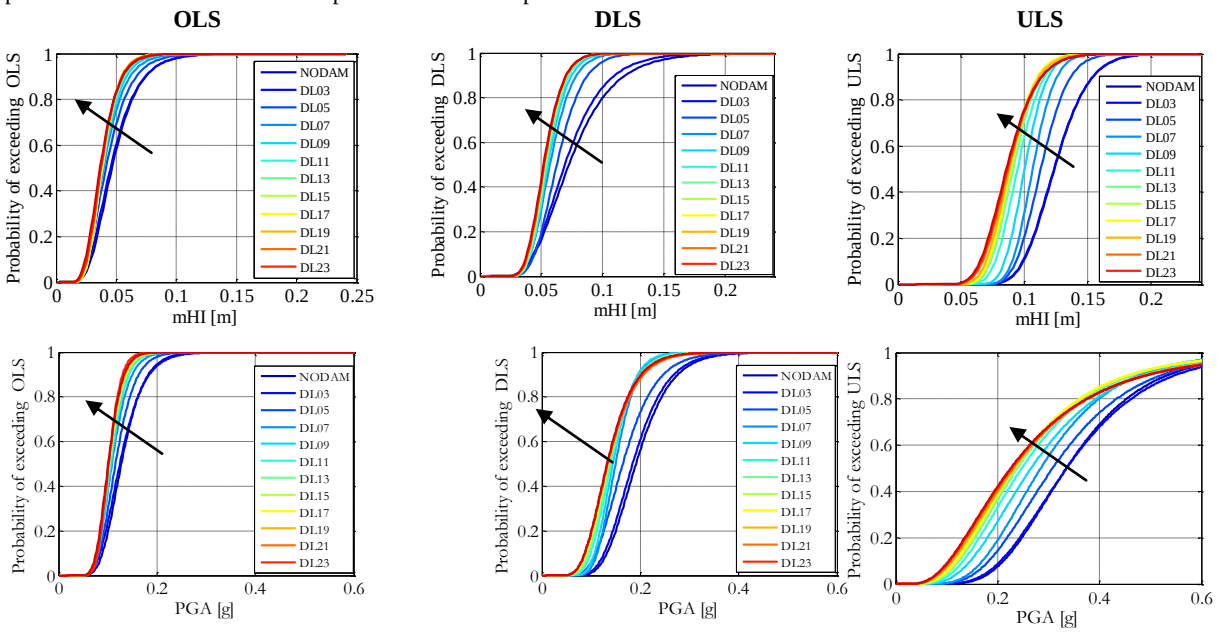

Figure 9: ***State-dependent fragility curves for different levels of pre-existing damage, for the three considered limit states (OLS, DLS and ULS from left to right), expressed in terms of modified HI (top) and PGA (bottom). The black arrows indicate the effect of increasing pre-existing damage.***

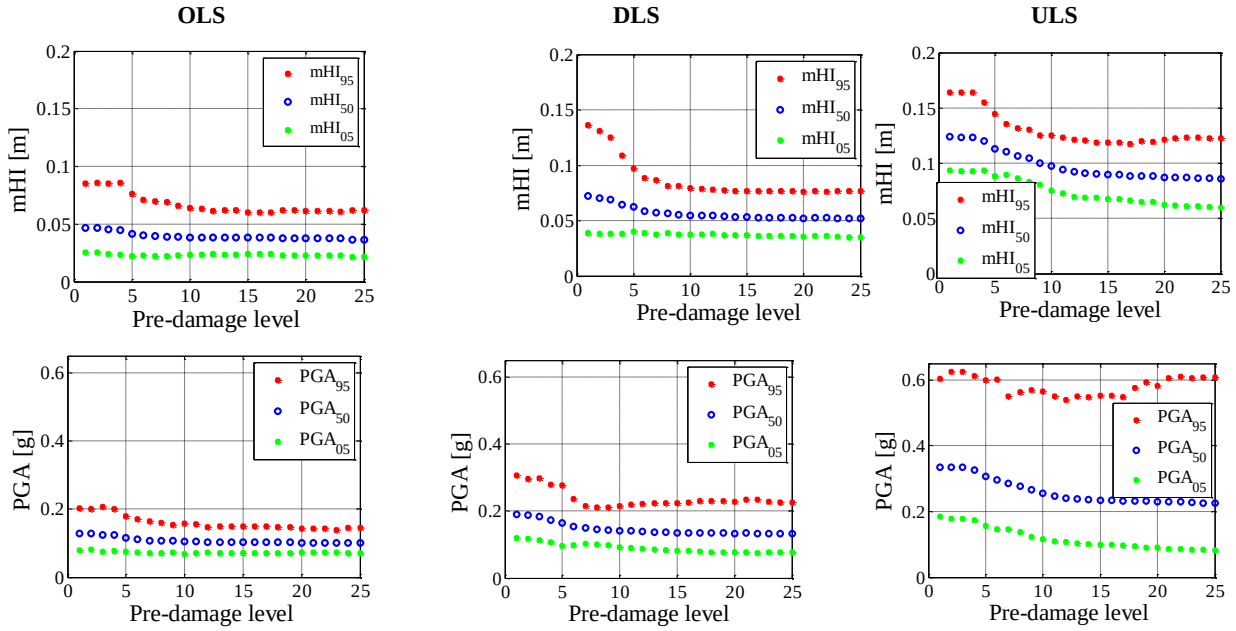

Figure 10: ***Evolution of the IM thresholds (mHI on the top and PGA on the bottom) corresponding to 50% (blue circles, middle), 95% (red solid markers, top) and 5% (green solid markers, bottom) probability of exceeding of OLS, DLS and ULS (from left to right), with increasing levels of pre-existing damage.***

4. DAMAGE EVOLUTION DURING THE CANTERBURY EARTHQUAKE SEQUENCE

The effect of cumulated damage on the seismic response of the previously presented unreinforced masonry building prototype was also studied with reference to a real sequence of events. In particular, the seismic activity recorded in the region of Canterbury (NZ) between September 2010 and January 2012 was selected for this study. The response of the structure was calculated both considering and neglecting the cumulated damage due to repeated events, in order to understand the influence of previous and cumulated damage on the vulnerability of the building.

The cumulated structural damage was captured by the displacement demand calculated for the SDOF model previously used for the derivation of state-dependent fragility curves. This calculated seismic demand is meant to represent the deformation demand imposed to an unreinforced clay masonry buildings existing in Canterbury, in the area of the station which recorded the ground motions used for the analyses.

4.1. Selected sequence of records

As already mentioned, the selected seismic sequence corresponds to the events occurred in the region of Canterbury (New Zealand) in the period of time from September 2010 to January 2012. During this time, a significant number of seismic events was recorded and, among those, the 20 strongest events (in terms of M_w), recorded by a single station, were selected [46].

For an easier interpretation of the results, the sequence of the 20 records is divided into 8 sub-sequences, each one corresponding to a relatively short period of time and including a mainshock and possible foreshocks and/or aftershocks that occurred during that period. For each sub-sequence, the mainshock is identified as the earthquake with the largest M_w. For example, the first and second sub-sequences correspond to the events of the 4th of September 2010 (Darfield earthquake and aftershocks) and the 22nd of February 2011 (Christchurch earthquake and aftershocks). The two horizontal components of the ground motion records were separately used, for a total of 2 sequences of 20 records each (40 records total).

These events were recorded by a large number of accelerometric stations spread over the area affected by the seismic sequence.

The large majority of the masonry building stock was located in the Christchurch Central Business District (CBD), where very strong shaking (with associated high values of PGA) were recorded during the February 2011 events [47]. This led to very high seismic demands, well beyond typical masonry buildings' capacity, as reflected by the significant number of collapses observed (see Figure 11 for some examples) [4].

Figure 11: ***Examples of severe damage and collapse of masonry buildings in the CBD area, Christchurch – Lee Campbell (left, http://leelcampbell.wordpress.com) and courtesy of Ilaria Senaldi (right).***

This application aims at investigating the cumulative effect of damage due to subsequent events, as well as the impact of aftershocks and foreshocks on the seismic vulnerability of masonry buildings. To this aim if a structure rapidly approaches collapse, possibly even in a single event, it is not possible to study the accumulation of damage over the whole earthquake sequence. For these reasons, records obtained from stations located in the CBD were not a suitable choice for the purposes of this application, as they would immediately lead to the collapse of the case study building, hindering the analysis of the effects of cumulated damage.

The records of the Riccarton High School station were eventually selected. One of the reasons is that the records of the mainshocks of the different events recorded at this station have comparable intensities and the aftershocks and foreshocks are not too small compared to the so-called mainshocks, hence inducing some additional damage to the structure.

Table 1 summarises some details of the selected ground motion records, whereas Figure 12 reports the values of mHI of the two horizontal components of shaking (named NS and EW, since they approximately correspond to the North-South and East-West directions, respectively), recorded at the Riccarton High School station. It can be noted that the events of the February 2011 sequence (events 4 to 6) have the highest mHI values, but they are still comparable to the other main events. Also, some foreshocks and aftershocks producing significant shaking at the site can be identified (e.g. records 12 and 15).

Table 1. Characteristics of the selected ground motions recorded at the Riccarton High School station.

				Modified Housner Intensity [m]		**PGA [g]**	
	record #	**Date**	M_w **[-]**	**NS** direction**	**EW** direction**	**NS** direction**	**EW** direction**
Sub-sequence 1	**1***	**04/9/2010**	**7.20**	**0.0997**	**0.1149**	**0.189**	**0.219**
	2	6/9/2010	5.00	0.0151	0.0167	0.033	0.033
	3	7/9/2010	4.80	0.0149	0.0172	0.030	0.033
Sub-sequence 2	**4**	**22/2/2011**	**6.20**	**0.1367**	**0.1447**	**0.293**	**0.250**
	5	22/2/2011	5.50	0.152	0.0925	0.253	0.184
	6	22/2/2011	5.60	0.1214	0.1137	0.232	0.215
Sub-sequence 3	**7**	**16/4/2011**	**5.00**	**0.0334**	**0.0294**	**0.090**	**0.062**
Sub-sequence 4	**8**	**10/5/2011**	**4.90**	**0.029**	**0.0322**	**0.069**	**0.074**
Sub-sequence 5	9	6/6/2011	5.10	0.0273	0.0241	0.072	0.045
	10	13/6/2011	5.30	0.0384	0.0494	0.073	0.091
	11	**13/6/2011**	**6.00**	**0.081**	**0.0941**	**0.188**	**0.189**
	12	21/6/2011	5.20	0.0833	0.0998	0.179	0.210
	13	22/7/2011	4.70	0.089	0.088	0.020	0.017
Sub-sequence 6	14	9/10/2011	4.90	0.0219	0.0189	0.040	0.049
Sub-sequence 7	15	23/12/2011	5.80	0.0666	0.0902	0.145	0.173
	16	23/12/2011	5.24	0.0118	0.0129	0.025	0.025
	17	23/12/2011	5.40	0.0169	0.0163	0.036	0.043
	18	**23/12/2011**	**5.90**	**0.0699**	**0.0700**	**0.155**	**0.153**
Sub-sequence 8	**19**	**2/1/2012**	**5.57**	**0.0186**	**0.0233**	**0.037**	**0.056**
	20	7/1/2012	5.19	0.0172	0.0204	0.035	0.055

*bold lines correspond to mainshocks of each sub-sequence.

**The direction indicated as "NS" corresponds to N86W, whereas "EW" corresponds to S04W.

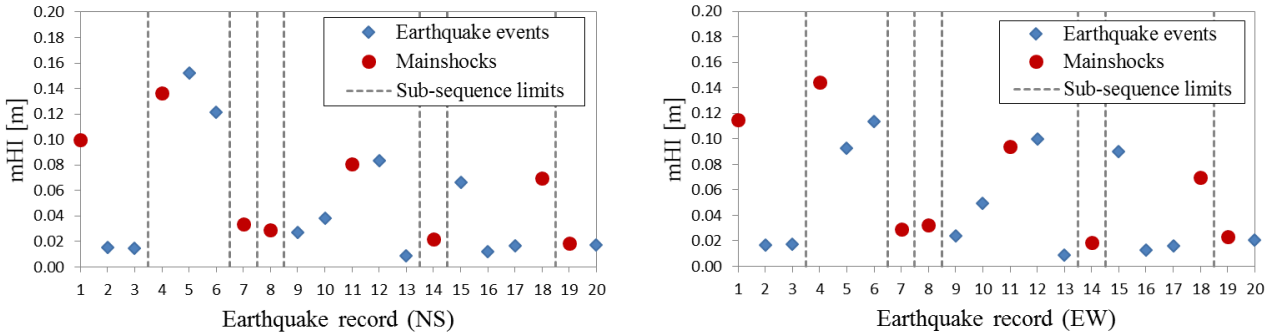

Figure 12: ***Modified Housner Intensity values of the selected records for the two horizontal directions of ground motion.***

4.2. Damage assessment considering separate sub-sequences of events

The seismic demand imposed to the structure by the 8 previously discussed sub-sequences of shocks was derived by means of time-history analyses with the SDOF model, both considering only the main shock of each sub-sequence and considering the complete sub-sequence. In both cases, analyses were performed with an undamaged model. The results corresponding to both cases are presented in Figure 13. In the same figure, the limit state displacement thresholds are shown for a better interpretation of the displacement demand.

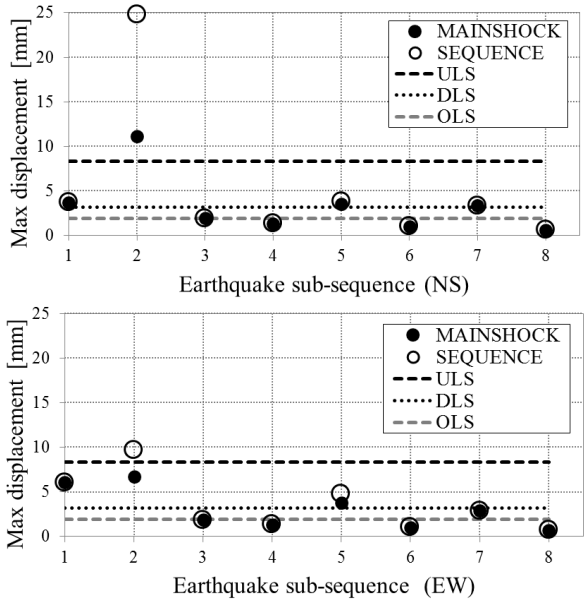

Figure 13: ***Displacement demand of the undamaged structure considering only the mainshocks of each sub-sequence and also considering the complete sub-sequences.***

The comparison of the seismic demand resulting from considering only the mainshocks and by considering the complete sub-sequences allows one to examine whether including foreshocks and/or aftershocks in a sequence of earthquake events affecting an undamaged structure leads to a different seismic demand with respect to that derived from the analysis of the mainshocks only. As shown in Figure 13, considering only the mainshock of sub-sequences 1, 7 and 8 provides the same value of maximum displacement that would be obtained by considering the entire sub-sequence, with records both in the NS and EW direction. This is not the case for sub-sequences 2 and 5, for which considering only the mainshocks leads to a lower value of displacement demand. This is particularly evident for the case of sub-sequence 2 and for analysis with records in the NS direction. The reason why different sub-sequences produce such different results is evident in Figure 12, showing that, for example for the 2nd sub-sequence (February 2011), the aftershocks have mHI values comparable with that of the main event, in particular for the records in the NS direction. Therefore, the maximum displacement demand is significantly increased when the entire sub-sequence is considered (i.e. when aftershocks are included in the analysis).

4.3. Cumulative damage assessment considering the whole sequence of events

In order to study the effect of cumulated damage, the maximum displacement demand induced to the case study building was evaluated for the whole sequence of earthquake events. The building model was exposed to subsequent earthquakes in order to simulate the response of a structure experiencing all the events of the selected sequence (i.e. from September 2010 to January 2012) one after the other.

Three cases were considered and the corresponding results are shown in Figure 14 in terms of maximum displacement demand obtained from the time-history analyses.

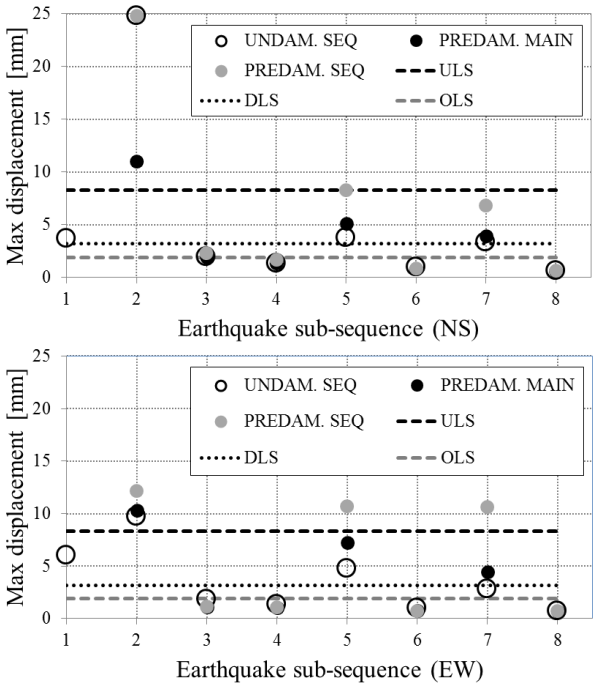

Figure 14: ***Displacement demand of the undamaged structure considering complete sub-sequences and of the pre-damaged structure considering two cases: mainshocks only and complete sub-sequences.***

In the first case (solid black circles in the figure) the pre-damaged model was exposed only to the main shocks of each sub-sequence (8 events in total); in the second case (solid grey circles), the pre-damaged model was exposed to the complete sequence of 8 sub-sequences (20 events in total). Finally, the third case (empty black circles) corresponds to the undamaged building, subjected to the entire sequence. The comparison of the results shows that, for some events, consideration of cumulating damage increases the seismic demand. This increase is more evident for the results of analyses with the EW components of the records, for which the 2nd sub-sequence is not significantly stronger than the others, as it is instead the case for the NS records. There is also an evident increase in displacement demand for the case in which the entire sequences of shaking (not only main shocks) are applied to the structure that was already subjected to the previous sub-sequences.

4.4. Analysis of the results obtained by applying the Christchurch sequence of records

The above preliminary results support the idea that pre-existing damage affects the response of a building subjected to a subsequent event only if the deformations experienced exceed a deformation threshold related with a significant limit state, which can be for example the DLS. The attainment of DLS corresponds indeed to the initiation of degradation of the structural response and the presence of permanent deformations.

Another conclusion supported by these preliminary results is that in order to have a difference in the seismic demand evaluated from time-history analyses considering the complete sequences and the demand from considering only the mainshocks, the aftershocks (or foreshocks) should have a significant intensity. This intensity can be described by a threshold of mHI, which varies from building to building and also depends on the characteristics of the applied records.

Looking at the results of this application, the threshold can be found somewhere between mHI equal to 0.04 and 0.06 m. This threshold is not independent from the state of the structure and it seems to decrease as the level of pre-existing damage increases.

This relation between the modified Housner intensity threshold and the level of pre-existing damage is somehow consistent with the trend observed in the results obtained in the derivation of state dependent fragility curves (Figure 10).

4.5. The academic case of an URM building erected on March 2011

In the preliminary results previously presented, the strong motions of the 22nd of February 2011 were prevailing in the real sequence and hence dominated the cumulated damage. As an academic exercise, the simulation was repeated considering only the earthquakes occurred after February 2011.

The exercise addresses a clay-brick URM building hypothetically erected during March 2011. The building model was subjected to the earthquake sequences occurring from March 2011 to January 2012 (13 strong events in total). The seismic demand was calculated by assuming that each earthquake in the sequence affects the previously undamaged structure and, then, for the structure experiencing all the subsequent events (with cumulative damage). The displacement demand obtained for both the undamaged and cumulatively damaged structure is shown in Figure 15. The dashed line in the figure shows the maximum displacement demand experienced by the structure during the occurrence of the subsequent earthquake events.

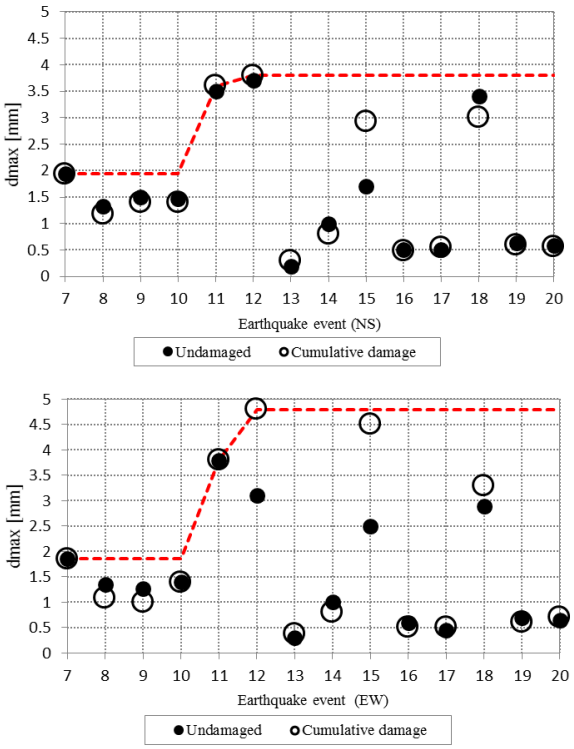

Figure 15: Comparison of displacement demand of undamaged structure and structure subjected to cumulative damage due to the earthquake sequence.

By looking at the results obtained from analyses performed considering the EW records, a change in the behaviour can be noted after the structure experiences event number 11. After this point, the maximum displacement demand related with the cumulative damage case is increased with respect to the previously undamaged structure. In particular, for the EW records, a significant difference in the displacement demand for the two cases can be observed for event number 15. In this case the pre-damaged structure has a maximum displacement demand of 4.5 mm, whereas the intact structure has a displacement demand of 2.5 mm. This indicates that there is a displacement level (in this case induced by event number 11 and resulting between 3.5 and 4.0 mm), whose exceedence modifies the response to the following shocks, making the displacement demand significantly different from that of the undamaged model. This displacement threshold can be related with the attainment of the maximum shear resistance and the beginning of the degrading response.

The results of analyses for the NS records show that in this case the degradation of the response is probably triggered after event number 14.

It can also be noted that, even after this threshold has been passed, the response of the structure to the less severe earthquakes (with values of Modified Housner Intensity smaller than 50 mm) is similar for the undamaged model and the pre-damaged model, showing that it is independent from the level of damage due to the previous events.

Figure 16 shows the time-history of the displacement demand during the entire considered sequence of events (EW records) and a zoom of the vertical axis of the same plot. The residual displacements on the structure due to the different events can be easily noted. Most of these residual displacements are of modest entity (some fractions of millimetre). Even for the most significant permanent displacements (still smaller than 0.1 mm), their final effect is compensated by their oscillating sign, which depends on the prevailing sign of the peaks of each accelerogram.

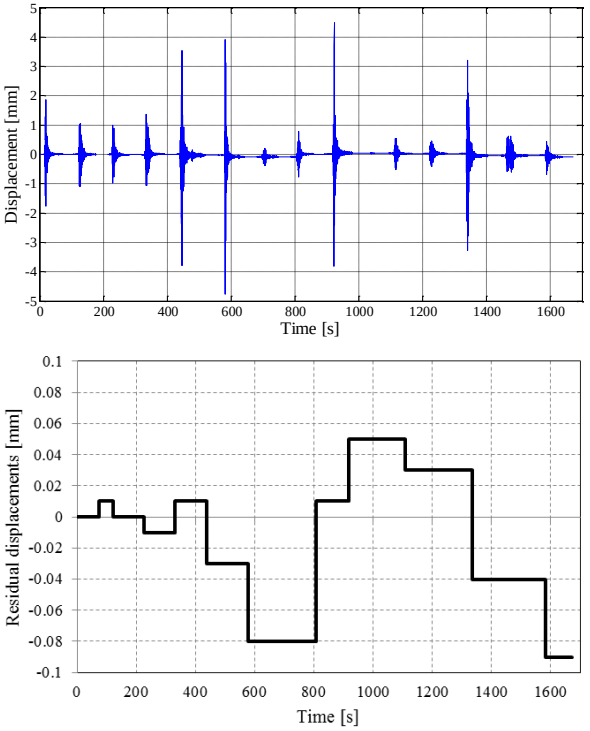

Figure 16: ***Time-history of the displacement demand during the entire considered sequence of events (top) and residual displacements (bottom) – EW records.***

Another conclusion supported by these preliminary results is that in order to have an increase of the peak displacement, the event should have mHI exceeding a given threshold. Figure 17 shows the increase of the maximum displacement experienced by the structure, as a function of the mHI of the different records. It can be noted that the displacement increases only in case of records with values of mHI higher than that causing the previous peak of displacement. In other words, it is possible to have an increment of damage in the structure only for increasing intensity values. This result indicates that, in case of a sequence in which the strongest shock (in terms of the selected IM) is the first event, consideration of cumulative damage does not seem to change the results with respect to considering only the mainshock, provided that the IM is well correlated to displacement demand. This is not true if the strongest shock occurs after damaging foreshocks.

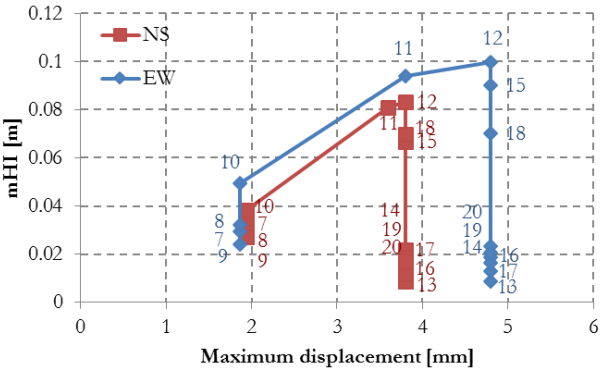

Figure 17: ***Variation of the maximum displacement demand experienced by the building for different values of mHI. The numbers refer to the record numbers, as in Table 1.***

5. CONCLUSIONS

This paper proposes an analytical approach for the derivation of fragility curves for masonry buildings, accounting for pre-existing damage states due to previous shaking. These state-dependent fragility curves are obtained from nonlinear dynamic analyses of an equivalent single-degree-of-freedom nonlinear model, with a large database of unscaled records. The applicability of the proposed methodology is shown with reference to a single case study building. Although the numerical results presented in the paper refer to this specific prototype, the approach is general and it is believed that some of the considerations obtained from this study can have a general validity.

The consideration of the effect on vulnerability of cumulated damage is in many cases important, particularly during a seismic sequence or in the case of different seismic events affecting an unrepaired building stock. In particular, in the case where building tagging is necessary right after an event and before a possibly occurring aftershock, it is important to have a quantitative estimate of the increased vulnerability of a structure, due to the damage already present in the building. These state-dependent fragility curves can hence constitute a useful tool for a quick quantification of this vulnerability when a large number of structures of similar typology need to be assessed in a short time.

The proposed procedure for deriving state-dependent fragility curves can also be combined with studies on the evolution of the structural state (including deterioration due to ageing) in the framework of time-dependent risk assessment. In this work, the state of the structure is considered only as a function of previous damage due to earthquake events experienced by the structure, whereas the effect of ageing is neglected.

The probability of structures previously exposed to earthquake events to exceed limit states' thresholds in subsequent events is a function of both the intensity of these events (measured in this work in terms of modified Housner Intensity and PGA) and the cumulated damage level. Intensity measure thresholds representing the attainment of limit states were studied as a function of the displacements characterizing the levels of pre-existing damage. The aforementioned thresholds decrease as the levels of pre-existing damage increase, with a similar trend for all the considered limit states.

The results obtained for the considered case study building show that the seismic demand imposed on structures could be evaluated in probabilistic terms, simply as a function of the intensity of the earthquake events that they have already experienced, without the need to perform any specific dynamic analysis. To this aim, the comparison of the fragility curves calculated in terms of PGA and of modified Housner Intensity showed that the latter intensity measure is better correlated with the evolution of damage, for the three limit states considered.

The proposed simplified SDOF model was also used for an application using the real earthquake sequence of Canterbury (New Zealand) during 2010-2012. This study highlighted the importance of considering the complete sequence of earthquakes (including foreshocks, mainshocks and aftershocks) in the damage assessment of masonry structures. This was captured by the significant differences obtained in terms of displacement demand derived when considering the entire sequence of events, rather than only the main events.

As observed by looking at the evolution of the derived analytical fragility curves, the probability of exceeding significant limit states in the case of events affecting previously damaged structures is a function of both the intensity of the event and the level of pre-existing damage. Similarly, for the case of an earthquake sequence, the

maximum displacement demand experienced by the structure depends on the ground motion severity and the cumulated previous damage. Moreover, the results obtained for the real sequence showed that, in this case, a damage increment can be observed only for events with values of intensity measures higher than those that have caused the pre-existing damage state.

Based on the results obtained in this work, the presence of some inconsistency in the approach currently used for the derivation of empirical fragility curves could be suspected. In the derivation of empirical fragility curves, the observed damage typically correspond to the final cumulated damage due to all the events that occurred before the survey is carried out. These damages are usually correlated with a synthetic representation of the seismic action, which typically corresponds to the parameters of the mainshock and does not take into any account the occurrence of multiple shocks hitting the same building stock. However, these empirical fragility curves are often combined with the results of probabilistic seismic hazard studies for the derivation of risk estimates. As the hazard is usually evaluated based on a declustered earthquake catalogue (from which foreshocks and aftershocks are removed), in order to have a realistic estimate of risk (which obviously should include the risk due to the entire seismic sequence), it seems appropriate to combine the mainshock hazard with empirical fragility curves correlating a ground motion parameter referring only to the main event (to allow a consistent convolution with hazard) with the cumulated damage caused by the entire sequence.

ACKNOWLEDGMENTS

This work was carried out with the financial support of the EC-FP7 REAKT Project - Strategies and tools for Real Time EArthquake RisK ReducTion (www.reaktproject.eu).

The authors thank Professor Jason Ingham for inspiring the application to the Canterbury earthquake sequence and providing the necessary information. Three anonymous reviewers provided valuable suggestions and useful comments which significantly improved the quality of the presentation of the work.

REFERENCES

1. Rota, M., Penna, A. and Strobbia, C. (2008) “Processing Italian damage data to derive typological fragility curves”. *Soil Dynamics and Earthquake Engineering*. **28**(10-11): 933-947.
2. Rota, M., Penna, A., Strobbia, C. and Magenes, G. (2011) “Typological seismic risk maps for Italy“. *Earthquake Spectra* **27**(3): 907-926.
3. Penna, A., Morandi, P., Rota, M., Manzini, C.F., da Porto, F., Magenes, G. (2014) “Performance of masonry buildings during the Emilia 2012 earthquake”. *Bulletin of Earthquake Engineering*, doi:10.1007/s10518-013-9496-6.
4. Dizhur, D., Ingham, J., Moon, L., Griffith, M., Schultz, A., Senaldi, I., Magenes, G., Dickie, J., Lissel, S., Centeno, J., Ventura, C., Leite, J., Lourenco, P. (2011) “Performance of masonry buildings and churches in the 22 February 2011 Christchurch earthquake“. *Bulletin of the New Zealand Society for Earthquake Engineering* **44**(4): 279-296.
5. Senaldi, I., Magenes, G., Ingham, J.M. (2014) “Damage assessment of unreinforced stone masonry buildings after the 2010-2011 Canterbury earthquakes”. *International Journal of Architectural Heritage* (in press).
6. Vamvatsikos, D., Dolsek, M. (2011) “Equivalent constant rates for performance-based seismic assessment of ageing structures”, *Structural Safety* **33**(1): 8-18.
7. Fotopoulou, S.D., Karapetrou, S.T. and Pitilakis, K.D. (2012) “Seismic vulnerability of RC buildings considering SSI and aging effects”. *Proceedings of. 15WCEE*, Lisboa, PT. Paper No. 5789
8. Iervolino, I., Giorgio, M. and Chioccarelli, E. (2013) “Gamma degradation models for earthquake-resistant structures”. *Structural Safety **45**:* 43-58.
9. Baker, J.W., Cornell, C.A. (2008) “Vector-valued intensity measures incorporating spectral shape for prediction of structural response”, *Journal of Earthquake Engineering* **12**(4): 534-554.
10. Jalayer, F., Asprone, D., Prota, A. and Manfredi, G. (2011) “A decision support system for post-earthquake reliability assessment of structures subjected to aftershocks: an application to L’Aquila earthquake, 2009”. *Bulletin of Earthquake Engineering* **9**:997–1014.
11. Iervolino, I., Giorgio, M. and Chioccarelli, E. (2013) “Closed-form aftershock reliability of damage-cumulating elastic-perfectly-plastic systems”. *Earthquake Engineering Structural Dynamics* **43**(4): 613–625.
12. Luco, N., Bazzurro, P. and Cornell, A. (2004). “Dynamic versus Static Computation of the Residual Capacity of a Mainshock-Damaged Building to withstand an Aftershock”. Proceedings *13thWCEE* ,Vancouver, Canada.
13. Réveillère, A., Gehl, P., Seyedi, D., Modaressi, H. (2012). “Development of seismic fragility curves for mainshock-damaged reinforced-concrete structures”. Proceedings *15th WCEE*, Lisboa, Portugal.
14. Aschheim, M., Black, E. (1999) “Effects of prior earthquake damage on response of simple stiffness-degrading structures”. *Earthquake Spectra* **15**(1):1–24.
15. Amadio, C., Fragiacomo, M., Rajgelj, S. (2003) “The effects of repeated earthquake ground motions on the non-linear response of SDOF systems”. *Earthquake Engineering and Structural Dynamics* **32**(2):291–308.
16. Hatzigeorgious, G., Beskos, D. (2009) “Inelastic displacement ratios for SDOF structures subjected to repeated earthquakes”. *Engineering Structures* **31**(11): 2744–55.
17. Ryu, H., Luco, N., Uma, S.R. and Liel, A.B. (2011) "Developing fragilities for mainshock-damaged structures through incremental dynamic analysis". 9th Pacific Conference on Earthquake Engineering, *NZSEE*, Auckland, New Zealand, Paper No. 225.
18. Raghunandan, M., Liel, A.B., Luco, N., Ryu, H. and Uma, S.R. (2012) “Aftershock Fragility Curves and Tagging Assessments for a Mainshock-Damaged Building”. Proceedings *15th WCEE*, Lisboa, Portugal
19. Di Sarno, L. (2013) “Effects of multiple earthquakes on inelastic structural response”. *Engineering Structures*, **56**: 673–681.
20. Fragiacomo, M., Amadio, C., Macorini, L. (2004) “Seismic response of steel frames under repeated earthquake ground motions”. *Engineering Structures*: 2021–2035.
21. ATC (1998) *FEMA 306 - Evaluation of Earthquake-Damaged Concrete and Masonry Wall Buildings: Basic Procedures Manual*, Redwood City, Calif.
22. ATC (1998) *FEMA 307 - Evaluation of Earthquake-Damaged Concrete and Masonry Wall Buildings: Technical Resources*, Redwood City, Calif.

23. Rota, M., Zuccolo, E., Taverna, L., Corigliano, M., Lai, C.G., Penna, A. (2012) "Mesozonation of the Italian territory for the definition of real spectrum-compatible accelerograms". *Bulletin of Earthquake Engineering*. **10**(5): 1357-1375.
24. Corigliano, M., Lai, C.G., Rota, M. and Strobbia, C.L. (2012) "ASCONA: Automated Selection of COmpatible Natural Accelerograms". *Earthquake Spectra* **28**(3): 965-987.
25. Smerzini, C., Galasso, C. and Paolucci, R. (2013). "Ground motion record selection based on broadband spectral compatibility". *Earthquake Spectra*, doi: http://dx.doi.org/10.1193/052312EQS197M.
26. Mouyiannou, A., Rota, M., Penna, A., Magenes, G. (2014) "Identification of suitable limit states from nonlinear dynamic analyses of masonry structures". *Journal of Earthquake Engineering* **18**(2): 231 – 263.
27. Rota, M., Penna, A. and Magenes, G. (2010) "A methodology for deriving analytical fragility curves for masonry buildings based on stochastic nonlinear analyses". *Engineering Structures* **32**(5): 1312-1323.
28. Yeo, G.L., Cornell, C.A. (2009). "Post-quake decision analysis using dynamic programming". *Earthquake Engineering and Structural Dynamics* **38**(1): 79-93.
29. Galloway, B., Hare, J., Brunsdon, D., Wood, P., Lizundia, B., Stannard, M. (2014) "Lessons from the Post-Earthquake Evaluation of Damaged Buildings in Christchurch", *Earthquake Spectra* **30**(1): 451-474.
30. Russell, A.P., Ingham, J.M. (2010) "Prevalence of New Zealand's Unreinforced Masonry Buildings", *Bulletin of the New Zealand Society for Earthquake Engineering*, **43**(3): 182-201.
31. Derakhshan, H., Griffith, M.C., Ingham, J.M. (2013) "Out-of-plane behavior of one-way spanning unreinforced masonry walls", *Journal of Engineering Mechanics*, ASCE, **139**(4): 409-417.
32. Lagomarsino, S. (2014) "Seismic assessment of rocking masonry structures", *Bulletin of Earthquake Engineering*, DOI 10.1007/s10518-014-9609-x.
33. Penna A., Rota, M., Mouyiannou A. and Magenes G. (2013). "Issues on the use of time-history analysis for the design and assessment of masonry structures". *Proc. COMPDYN2013*, Kos Island, Greece, Paper No. 1327.
34. Magenes, G., Calvi, G.M. and Kingsley, G.R. (1995). "Seismic Testing of a Full-Scale, Two-Story Masonry Building: Test Procedure and Measured Experimental Response". *University of Pavia, Italy.*
35. Penna, A., Lagomarsino, S. and Galasco, A. (2014). "A nonlinear macro-element model for the seismic analysis of masonry buildings". *Earthquake Engineering and Structural Dynamics*, **43**(2): 159-179.
36. Lagomarsino, S., Penna, A., Galasco, A. and Cattari S. (2013). "TREMURI program: an equivalent frame model for the nonlinear seismic analysis of masonry buildings". *Engineering Structures* **56**: 1787-1799.
37. Mazzon, N., Valluzzi, M.R., Aoki, T., Garbin, E., De Canio, G., Ranieri, N., Modena, C. (2009) "Shaking table tests on two multi-leaf stone masonry buildings", Proc. 11th Canadian Masonry Symposium, Toronto.
38. Elmenshawi, A., Sorour, M., Mufti, A., Jaeger, L.G., Shrive, N. (2010) "Damping mechanisms and damping ratios in vibrating unreinforced stone masonry", *Engineering Structures* **32**(10), 3269–3278.
39. Graziotti, F. (2013) "Contributions towards a Displacement-Based Seismic Assessment of Masonry Structures". Ph.D. Dissertation, *UME School, Pavia.*
40. Italian Building Code (2008). DM 14.01. 2008: Norme Tecniche per le Costruzioni.
41. Costa, A.A., Penna, A., Magenes, G. (2011) "Seismic performance of Autoclaved Aerated Concrete (AAC) masonry: from experimental testing of the in-plane capacity of walls to building response simulation". *Journal of Earthquake Engineering*, **15**(1): 1-31.
42. Tondelli, M., Rota, M., Penna, A. and Magenes, G. (2012) "Evaluation of uncertainties in the seismic assessment of existing masonry buildings". *Journal of Earthquake Engineering* **16**(S1): 36-64.
43. Magenes, G., Penna, A. (2011) "Seismic design and assessment of masonry buildings in Europe: recent research and code development issues", Keynote paper, *Proceedings of the 9th Australasian Masonry Conference*, Queenstown, New Zealand, 585-603.
44. Housner, G.W. (1959). "Behavior of structures during earthquakes". *Journal of the Engineering Division*, ASCE, Vol**. 85**, No. EM14, 109-129.
45. Graziotti, F., Penna, A. and Magenes, G. (2013). "Use of equivalent SDOF systems for the evaluation of displacement demand for masonry buildings". *Proc. of VEESD 2013*, Vienna, Austria.
46. Bradley, B.A., Quigley, M.C., Van Dissen, R.J. and Litchfield, N.J. (2013) "Ground Motion and Seismic Source Aspects of the Canterbury Earthquake Sequence", *Earthquake Spectra*, **30**(1): 1–15.
47. Moon, L., Dizhur D., Senaldi, I., Derakhshan, H., Griffith, M., Magenes, G. and Ingham, J. (2014) "The demise of the URM building stock in Christchurch during the 2010/2011 Canterbury earthquake sequence", *Earthquake Spectra*, **30**(1): 253-276.